PNAS
www.pnas.org

Supplementary Information for

Structure of RNA polymerase complex and genome within a dsRNA virus provides insights into the mechanisms of transcription and assembly

Xurong Wang, Fuxian Zhang, Rui Su, Xiaowu Li, Wenyuan Chen, Qingxiu Chen, Tao Yang, Jiawei Wang, Hongrong Liu, Qin Fang, and Lingpeng Cheng

Correspondence to: Hongrong Liu, Qin Fang, and Lingpeng Cheng
Emails: hrliu@hunnu.edu.cn, qfang@wh.iov.cn, and lingpengcheng@mail.tsinghua.edu.cn

This PDF file includes:

Supplementary text
Figs. S1 to S10
Tables S1 to S2

www.pnas.org/cgi/doi/10.1073/pnas.1803885115

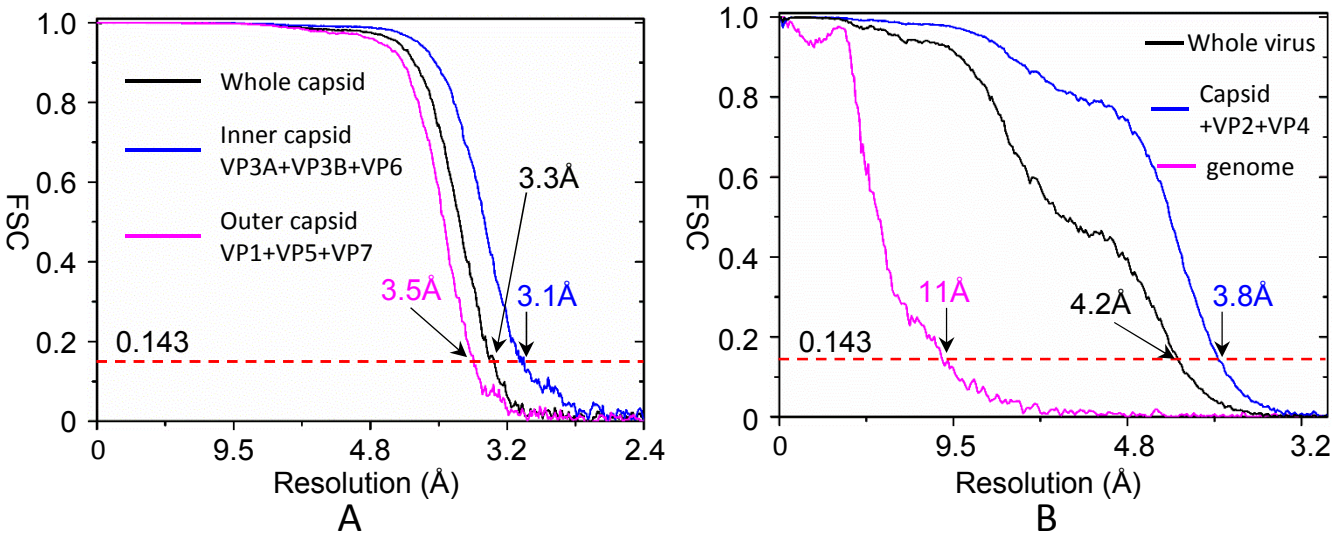

Fig. S1. Structural resolutions estimated by Fourier shell correlation. **(A)** The structural resolutions of the whole double-layered capsid, inner capsid, and outer capsid determined by icosahedral reconstruction are 3.3, 3.1, and 3.5 Å, respectively. **(B)** The structural resolutions of whole aquareovirus, capsid (including VP2 and VP4), and genome determined by symmetry-mismatch reconstruction are 4.2, 3.8, and 11 Å, respectively.

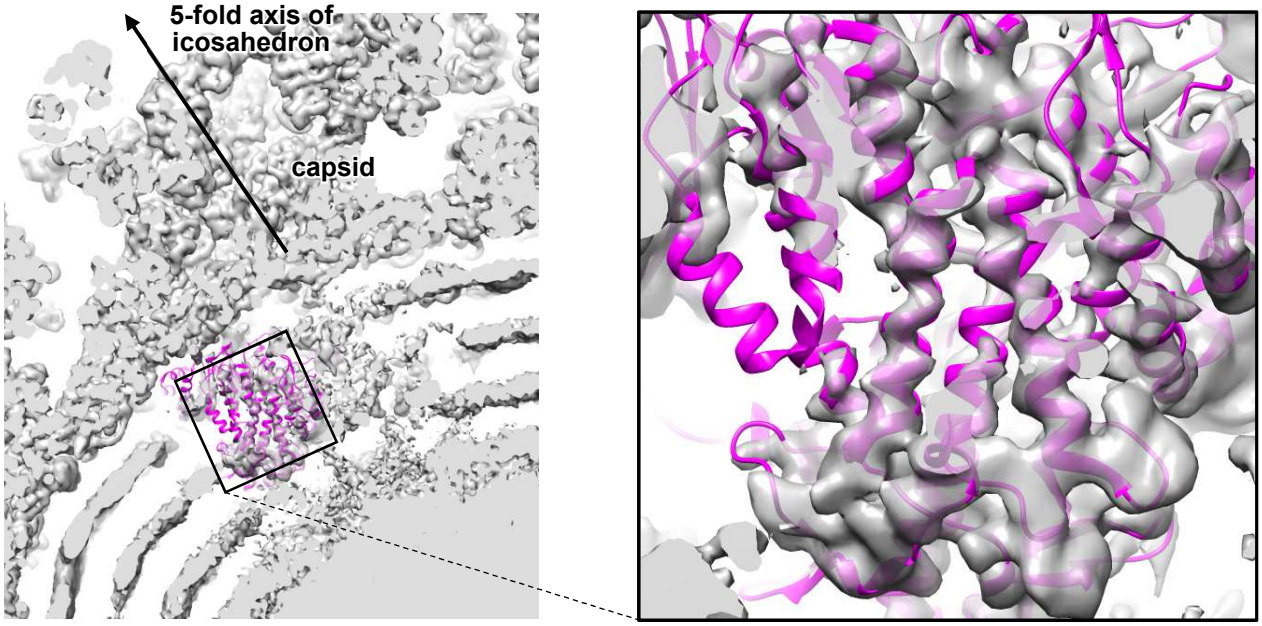

Fig. S2. Fit of crystal structure model of orthoreovirus λ3 into the density of VP4 in aquareovirus structure reconstructed by icosahedral reconstruction.

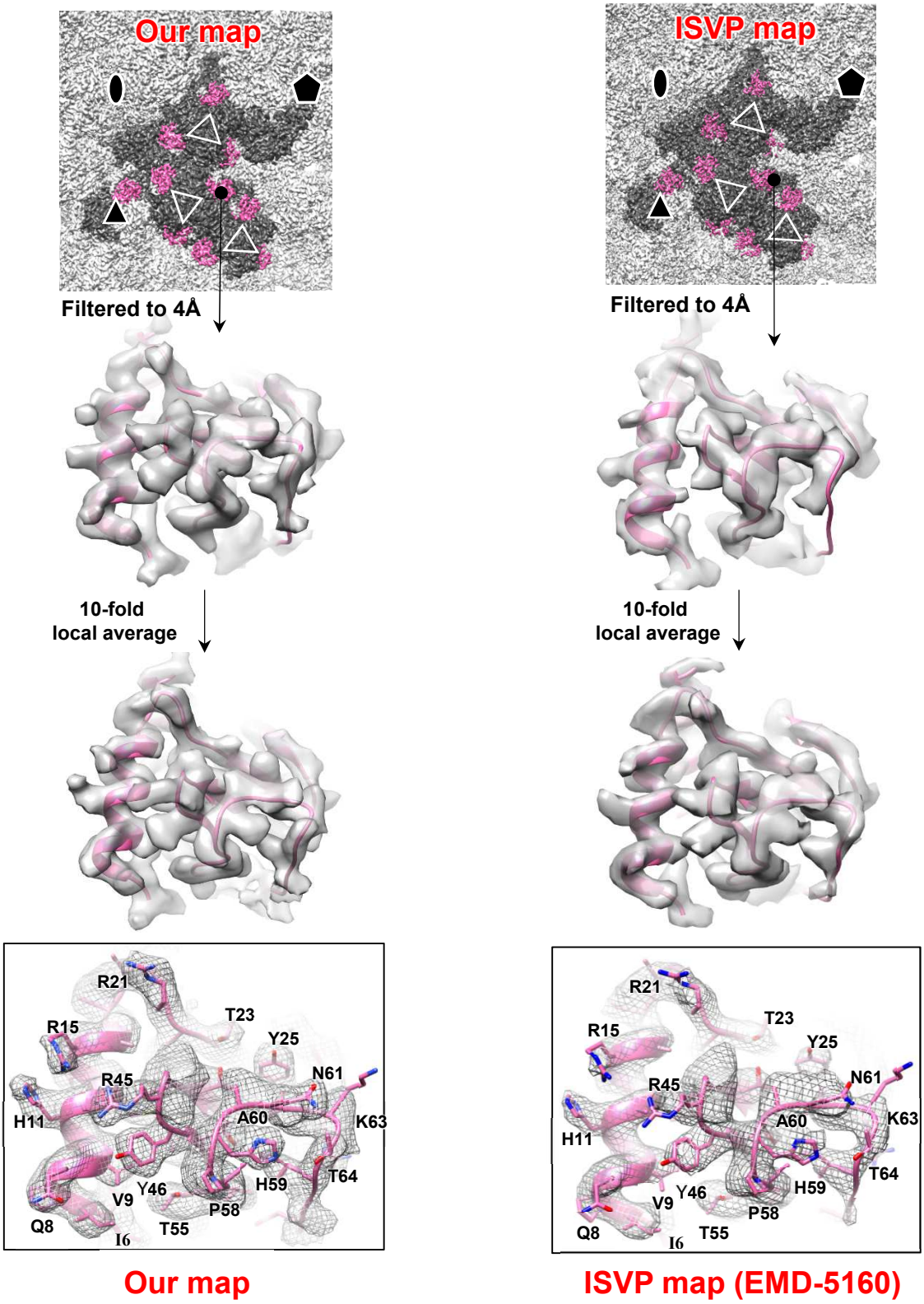

Fig. S3. The 10 VP7 structures in the icosahedral asymmetric unit, which are identified in our aquareovirus density map (left) and the aquareovirus ISVP density map (right) reported previously (Zhang et. al., *Cell*, 2010, 141, 472–82), are identical.

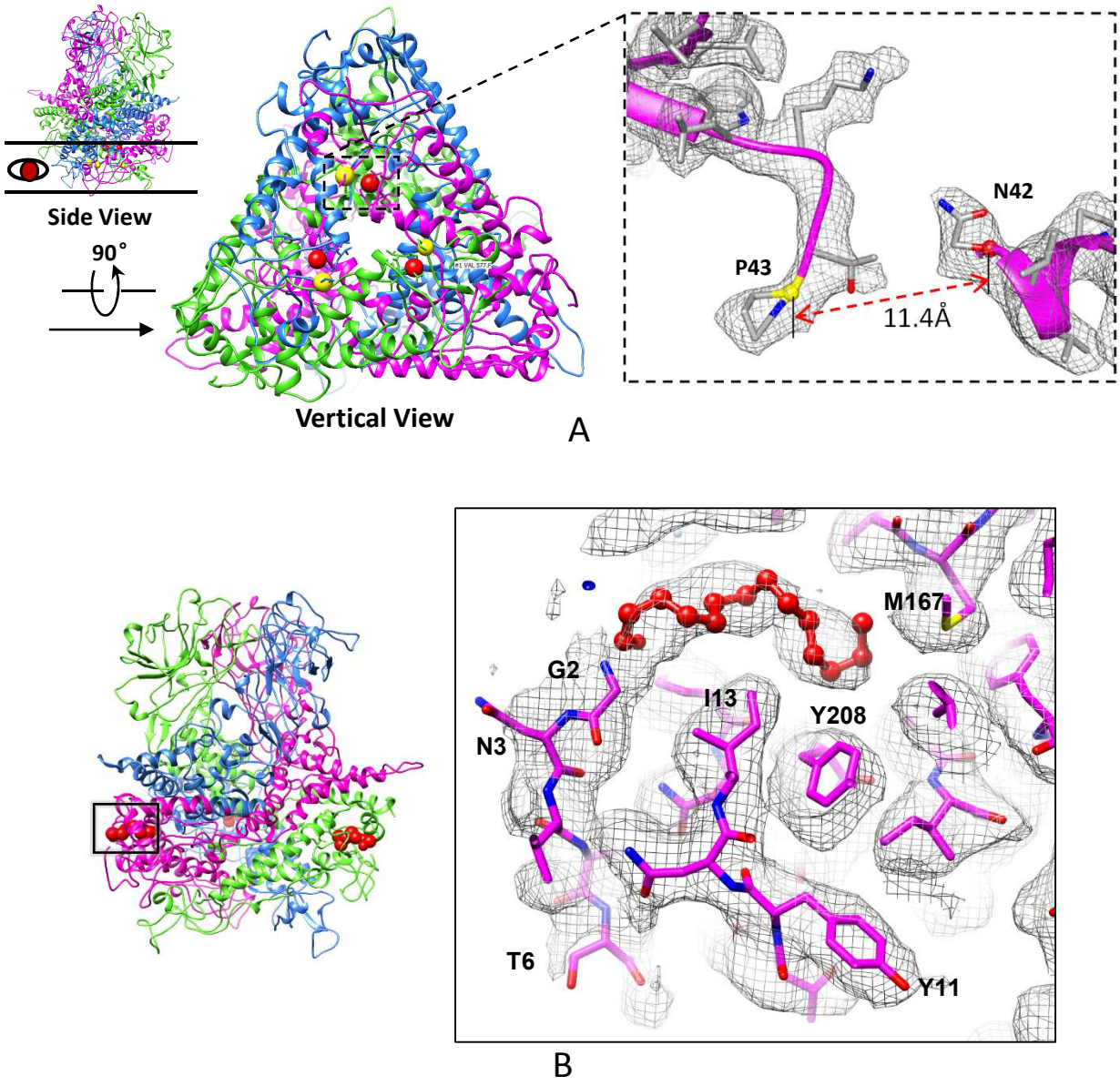

Fig. S4. Structure of VP5 trimer is clearly resolved in our aquareovirus structure. Our trimer structure (mesh) is identical to that in aquareovirus ISVP density map reported previously (Zhang et. al., *Cell*, 2010, 141, 472–82 (A) Cleavage site between Asn42 and Pro43 of our VP5 structure. (B) Myristoyl group linked to the N-terminus of our VP5 structure.

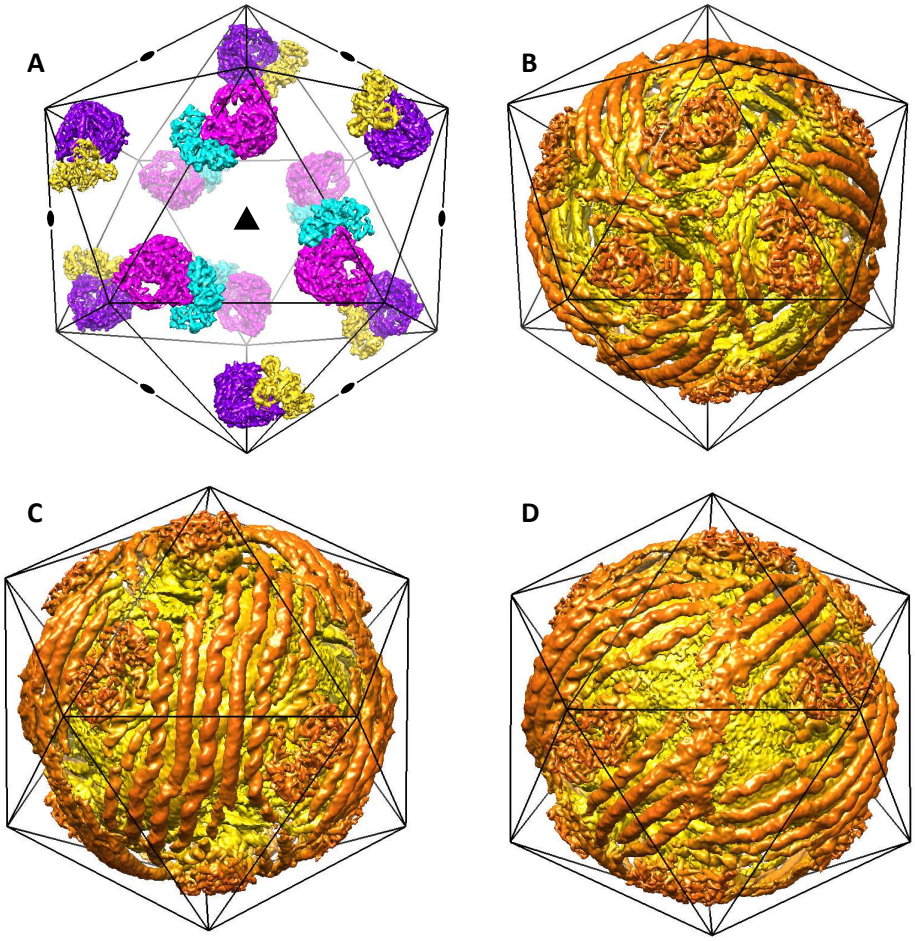

Fig. S5. Structure of the genomic RNA and VP2-VP4 complexes in aquareovirus. (A) The distribution of VP2-VP4 complex within the icosahedral capsid (viewed along the threefold axis). The threefold VP2 and VP4 are in magenta and cyan respectively. The twofold VP2 and VP4 are in purple and yellow respectively. The vertices of threefold axis (triangle) and two twofold axes (ellipses) are indicated. (B-D) The structures of genomic RNA and RdRp complexes viewed along the threefold and the two twofold axes.

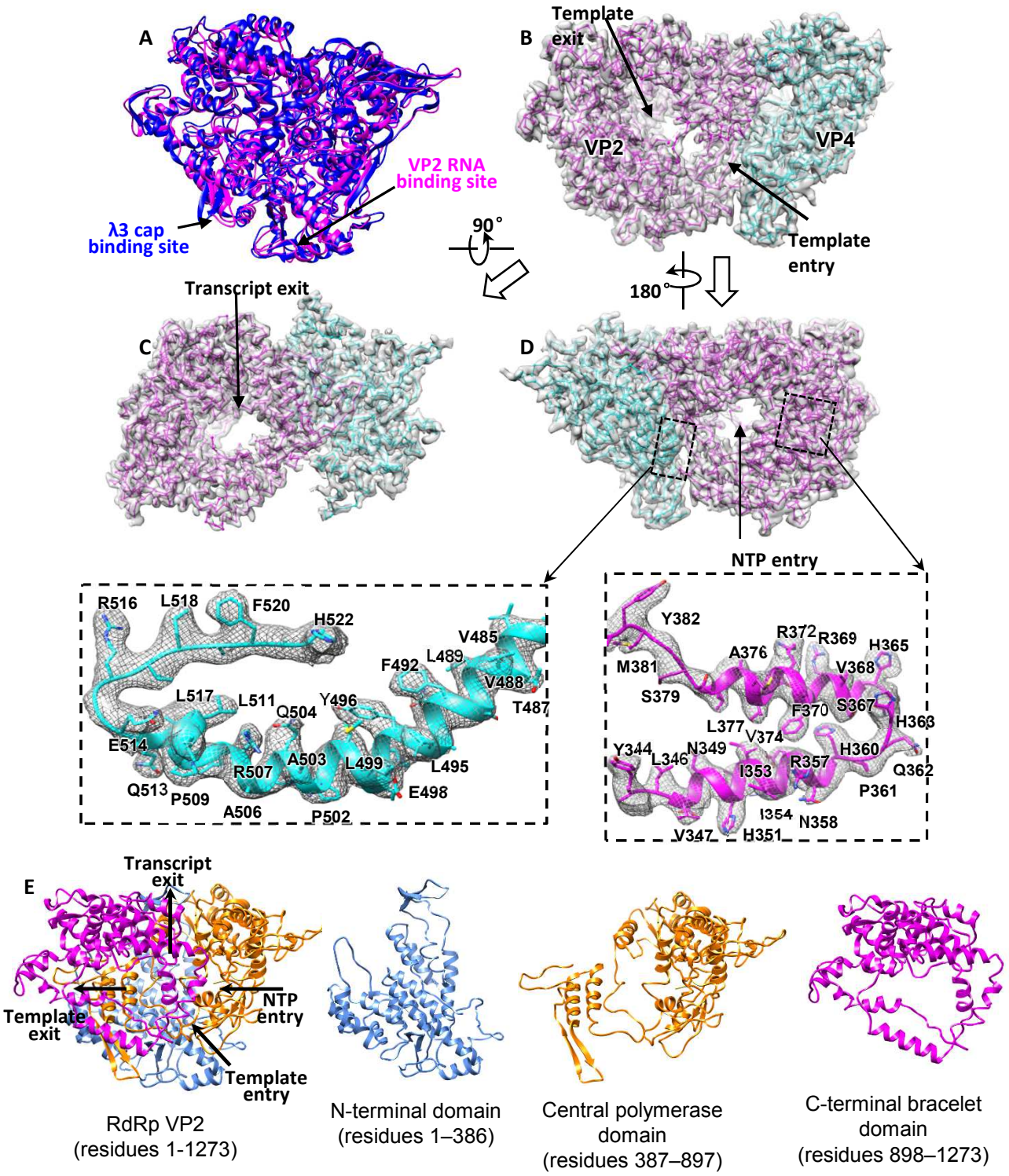

Fig. S6. Structure of RdRp VP2 and cofactor protein VP4. (A) Structural comparison between the aquareovirus VP2 (magenta ribbon) and orthoreovirus λ3 (blue ribbon) shows that they are almost identical. The cap binding site in λ3 and the RNA binding site in VP2 are indicated by arrows. (B), (C), and (D) Transparent views of the density map of VP2 and VP4 superimposed with their atomic model (only the backbone is shown). The VP2 and VP4 are in magenta and cyan respectively. Zoom-in views show that the side chains fit well with the density map. (E) Ribbon diagram showing the structure of VP2 and its three domains. The N-terminal, central polymerase, and C-terminal domains are in light blue, yellow and magenta, respectively.

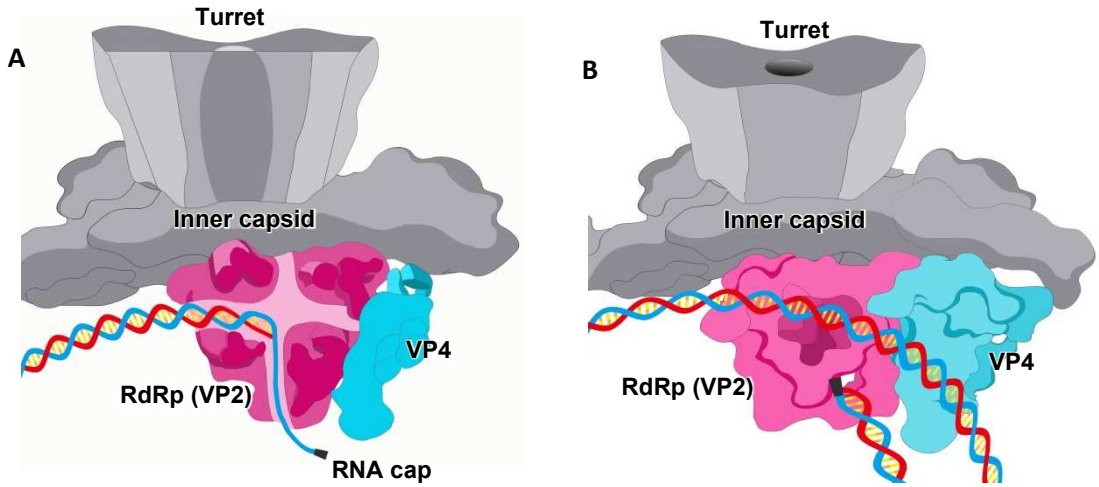

Fig. S7. Diagram of modes of RNA replication. (A) dsRNA is replicated from the plus-strand template RNA (blue strand). The four channels are shown in the same direction as those in Fig. 2B. (B) Interactions between dsRNA and RdRp-VP4 complex within the capsid after replication.

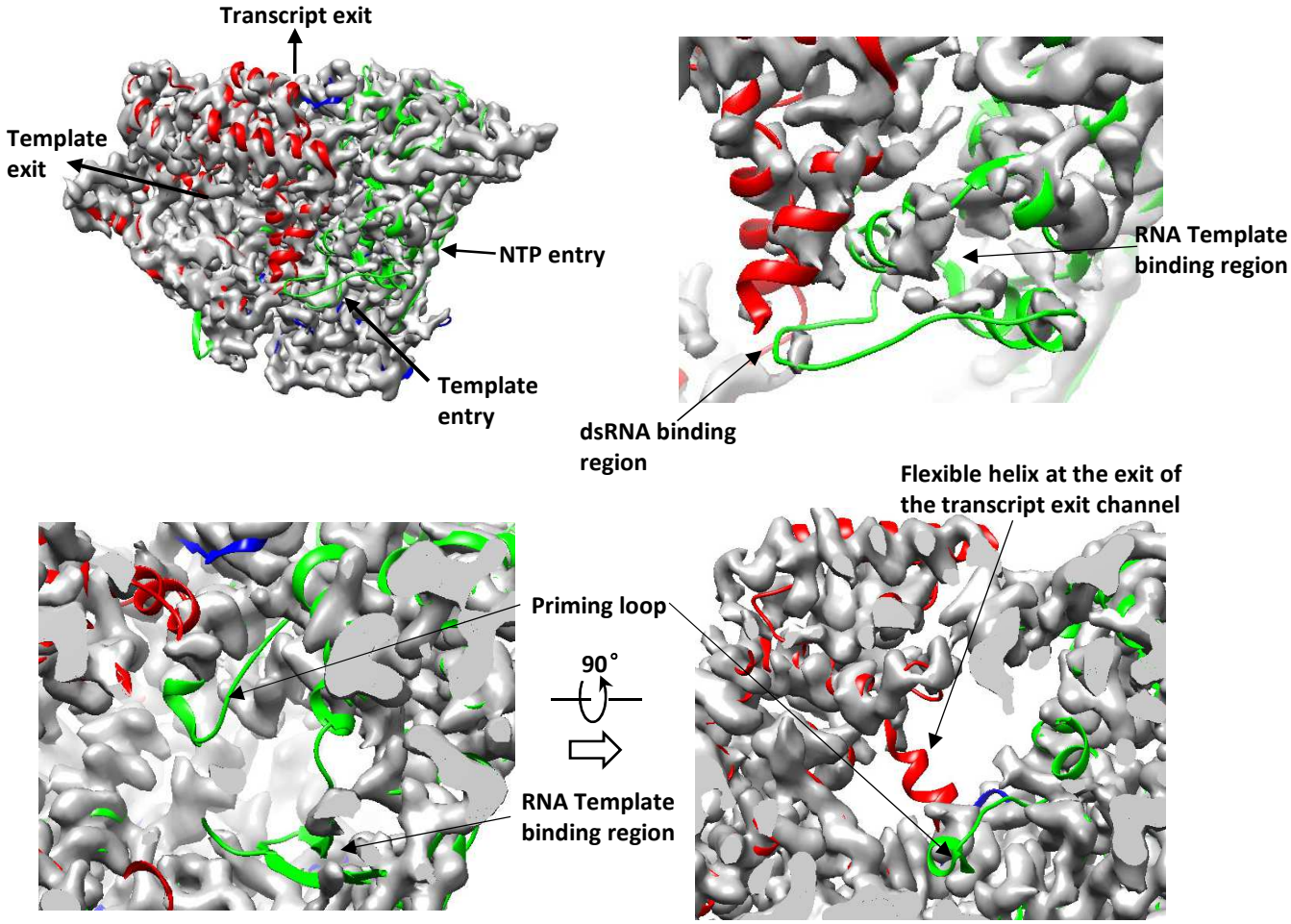

Fig. S8. Density map (gray) of aquareovirus VP2 superimposed with the atomic model of orthoreovirus λ3 (ribbon), in which N-terminal, polymerase, and bracelet domains are in blue, green, and red, respectively. The RNA template and product were not shown.

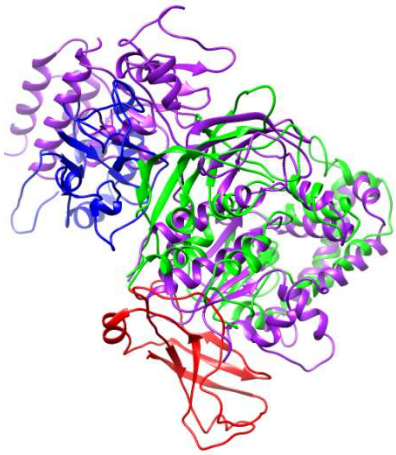

Fig. S9. Structural comparison between aquareovirus VP4 and cypovirus VP4. The structure of cypovirus VP4 is in purple. The N-terminal nodule domain, plate domain, and C-terminal domain are in blue, green, and red, respectively.

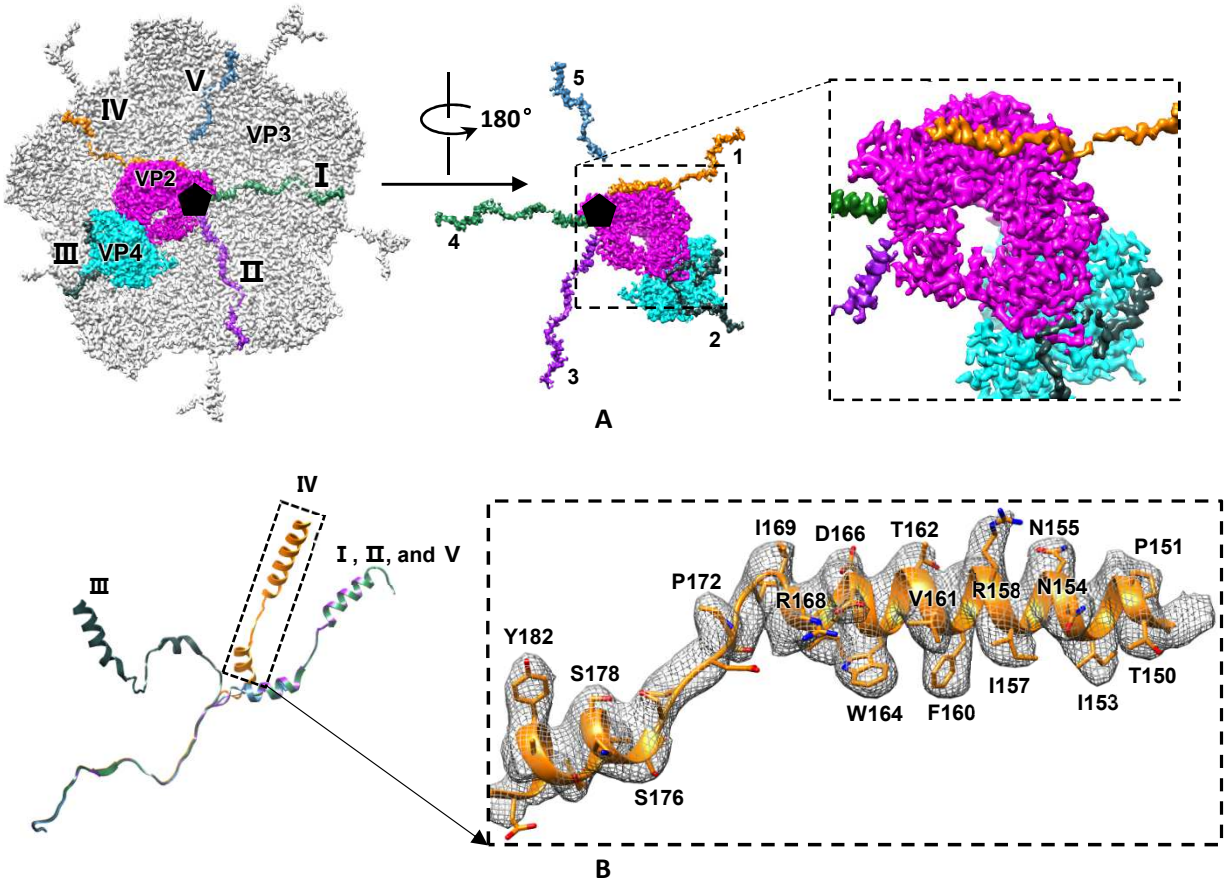

Fig. S10. Interactions among the N-termini of VP3A, VP2, and VP4. (A) Structure of the VP2-VP4 and the innermost capsid shell proteins viewed from inside. Five N-termini of VP3A are marked with I-V. (B) Left: superimpose of the five N-termini structures (ribbon). Right: the density map of a N-terminus (mesh) superimposed with its atomic model.

Table S1. Capsid proteins of aquareovirus, orthoreovirus, and cypovirus

Aquareovirus Protein (aa number) / Genome segment (bp) (GenBank accession)	Orthoreovirus Protein (aa number) / Genome segment (bp) (GenBank accession)	Cypovirus Protein (aa number) / Genome segment (bp) (GenBank accession)	Functions, location, and post-translational modification
VP1 (1299) / S1 (3949) (AH009795)	λ2 (1289) / L2 (3916) (EF494436)	VP3 (1058) / S4 (3262) (AF323784)	Guanylyl transferase and methylases; forms pentameric turret on the outer surface of the innermost capsid shell at each fivefold vertex.
VP2 (1274) / S2 (3877) (AH009795)	λ3 (1267) / L1 (3854) (EF494435)	VP2 (1225) / S2 (3854) (AF323782)	RdRp; on the inner surface of the innermost capsid shell under each fivefold vertex.
VP3 (1214) / S3 (3702) (AH009795)	λ1 (1275) / L3 (3901) (EF494437)	VP1 (1333) / S1 (4190) (AF323781)	Forms the innermost capsid shell.
VP4 (728) / S5 (2239) (AF403391)	μ2 (736) / M1 (2304) (EF494438)	VP4 (561) / S6 (1796) (AB030014)	NTPase; on the inner surface of the innermost capsid shell at each fivefold vertex and interacts with RdRp.
VP5 (648) / S6 (2019) (AF403392)	μ1 (708) / M2 (2203) (EF494439)	N/A	Membrane penetration protein, which is loacated in the outer capsid; myristoylated at N-terminus and autocleaved at Asn42-Pro43.
VP6 (412) / S8 (1296) (AF403394)	σ2 (418) / S2 (1331) (EF494442)	VP5 (448) / S7 (1501) (AB030015)	Clamper protein, which enhances the stability of innermost capsid shell; sits on innermost capsid shell. Cypovirus VP5 might be cleaved at Asn291-Ala292.
VP7 (276) / S10 (909) (AF403396)	σ3 (365) / S4 (1196) (EF494444)	N/A	Outermost protection protein, which is located on membrane penetration protein.
N/A	σ1 (455) / S1 (1416) (EF494441)	Unknown	Cell attachment protein, which is located on the turret at each fivefold vertex.

Table S2. Refinement and model statistics

Data collection			
EM	FEI 200 kV Technai Arctica, Falcon II camera		
Pixel size (Å)	0.932		
Defocus range (μm)	1.2~3.2		
Reconstruction	VP2	VP4	VP7
Final resolution (Å)	3.5	3.5	3.3
Refinement (phenix.real_space_refine)			
Residue numbers	1245	583	86
CC (model to map fit)	0.825	0.823	0.725
Validation			
R.M.S. deviation from ideal values			
Bonds (Å)	0.010	0.013	0.006
Angle (°)	1.000	1.160	1.532
Ramachandran plot statistics (%)			
Most favorable	86.7	81.3	86.6
Additionally allowed	11.8	15.9	13.4
Disallowed	1.5	2.8	0.0